

Accepted Manuscript

Wettability alteration of oil-wet carbonate by silica nanofluid

Sarmad Al-Anssari, Ahmed Barifcani, Shaobin Wang, Lebedev Maxim, Stefan Iglauer

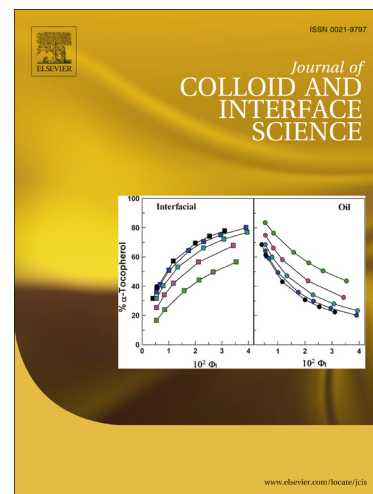
PII: S0021-9797(15)30222-8
DOI: <http://dx.doi.org/10.1016/j.jcis.2015.09.051>
Reference: YJCIS 20761

To appear in: *Journal of Colloid and Interface Science*

Received Date: 7 August 2015
Revised Date: 21 September 2015
Accepted Date: 21 September 2015

Please cite this article as: S. Al-Anssari, A. Barifcani, S. Wang, L. Maxim, S. Iglauer, Wettability alteration of oil-wet carbonate by silica nanofluid, *Journal of Colloid and Interface Science* (2015), doi: <http://dx.doi.org/10.1016/j.jcis.2015.09.051>

This is a PDF file of an unedited manuscript that has been accepted for publication. As a service to our customers we are providing this early version of the manuscript. The manuscript will undergo copyediting, typesetting, and review of the resulting proof before it is published in its final form. Please note that during the production process errors may be discovered which could affect the content, and all legal disclaimers that apply to the journal pertain.



Wettability alteration of oil-wet carbonate by silica nanofluid

Sarmad Al-Ansari^{1*}, Ahmed Barifcani^{1,2}, Shaobin Wang¹, Lebedev Maxim³, Stefan Iglauer²

¹*Department of Chemical Engineering, Curtin University, Kent Street, 6102 Bentley, Australia*

²*Department of Petroleum Engineering, Curtin University, 26 Dick Perry Avenue, 6151 Kensington, Australia*

³*Department of Exploration Geophysics, Curtin University, 26 Dick Perry Avenue, 6151 Kensington, Australia*

* corresponding author

Postal address: Curtin University, 26 Dick Perry Avenue, 6151 Kensington, Australia

Telephone: 0452544988

Email address: sarmad.al-ansari@postgrad.curtin.edu.au

sarmadfoad@yahoo.com

Wettability alteration of oil-wet carbonate by silica nanofluid

Sarmad Al-Ansari^{1*}, Ahmed Barifcani^{1,2}, Shaobin Wang¹, Lebedev Maxim³, Stefan Iglauer²

¹*Department of Chemical Engineering, Curtin University, Kent Street, 6102 Bentley, Australia*

²*Department of Petroleum Engineering, Curtin University, 26 Dick Perry Avenue, 6151 Kensington, Australia*

³*Department of Exploration Geophysics, Curtin University, 26 Dick Perry Avenue, 6151 Kensington, Australia*

* corresponding author

ABSTRACT

Changing oil-wet surfaces towards higher water wettability is of key importance in subsurface engineering applications. This includes petroleum recovery from fractured limestone reservoirs, which are typically mixed or oil-wet, resulting in poor productivity as conventional waterflooding techniques are inefficient. A wettability change towards more water-wet would significantly improve oil displacement efficiency, and thus productivity. Another area where such a wettability shift would be highly beneficial is carbon geo-sequestration, where compressed CO₂ is pumped underground for storage. It has recently been identified that more water-wet formations can store more CO₂.

We thus examined how silica based nanofluids can induce such a wettability shift on oil-wet and mixed-wet calcite substrates. We found that silica nanoparticles have an ability to alter the wettability of such calcite surfaces. Nanoparticle concentration and brine salinity had a significant effect on the wettability alteration efficiency, and an optimum salinity was identified, analogous to that one found for surfactant formulations. Mechanistically, most nanoparticles irreversibly adhered to the oil-wet calcite surface (as substantiated by SEM-EDS and AFM measurements). We conclude that such nanofluid formulations can be very effective as enhanced hydrocarbon recovery agents and can potentially be used for improving the efficiency of CO₂ geo-storage.

1. Introduction

The unique properties of designed nanoparticles have shown promising applications in a diverse range of fields, spanning from medicine,¹ drug delivery,² biology,³ food additives,⁴ polymer composite,⁵ metal ions removal,⁶ corrosion protection,⁷ heterogeneous catalysis,⁸ and improved surface properties⁹ to enhanced oil recovery,^{5,10} on which we focus here.

In enhanced oil recovery (EOR), one of the main challenges is hydrocarbon production from fractured limestone reservoirs. These reservoirs contain more than half of the known remaining oil reserves in the world,¹¹ and they are typically intermediate-wet or oil-wet.¹² Secondary recovery (conventional water flooding techniques) is inefficient and productivity is low: mainly oil from the fractures is produced as water does not spontaneously imbibe into

the oil-wet rock matrix;¹³ however, most oil is stored in the matrix,¹² and as a result only 10-30% of the oil is recovered.¹⁴

One mechanism, which can significantly improve oil production, is to render the oil- (or intermediate-) wet carbonate surfaces water-wet, so that water spontaneously imbibes into the rock and displaces the oil from the matrix pore space.¹⁵ Several methods have been suggested: surfactant flooding,^{13,14} polymer flooding,^{16,17} nanoparticle stabilized emulsions,¹⁸ various nanoparticle-surfactant-polymer formulations,¹⁹⁻²⁴ and nanofluids.²⁵⁻²⁸ Surfactant EOR has been tested at field scale, but efficiency proved to be poor.²⁹ However, when polymer was used as cosurfactant, oil recovery was enhanced significantly.²⁹ The other techniques have not been used at industrial scale as far as we are aware.

Furthermore a wettability change towards more water-wet would be greatly beneficial to Carbon Geo-Storage (CCS) projects, where oil-wet rock surfaces lead to dramatically reduced storage capacity and containment security.^{30,31} Specifically, higher water wettability has been shown to increase residual trapping capacities, at the reservoir scale³⁰, and at the core- or pore-scale (e.g. Spiteri et al. 2008³², Pentland et al. 2011³³, Iglauer et al. 2012³⁴ and Iglauer et al. 2011³⁵ versus Chaudhary et al. 2013³⁶). Moreover, higher structural trapping capacities are predicted for strongly water-wet systems.³¹

It is thus highly desirable to render such hydrophobic mineral surfaces strongly water-wet; the key to successful EOR and improved CCS is therefore to find formulations, which are very efficient in wettability alteration at very low concentrations (because of economical cost). The economic viability of these processes depends on crude oil prices and carbon tax.

Nanoparticle formulations can meet these requirements as they are active at low concentrations (e.g. compare Mahbul, et al.³⁷), and can migrate through the pore space of the reservoir and penetrate into even the smallest pores²⁴ – note that rock matrix pore sizes in limestone vary between 0.01-100 μm .³⁸ However, the efficiency of such formulations is a complex function of several factors, including the size and type of nanoparticles, nanofluid preparation and stability, the nature of the porous medium, thermo-physical and geological conditions and dwell time in the reservoir.^{39, 40} Despite the vital importance for limestone reservoirs globally, previous studies focused on sandstone formations,^{21,25,26,28,41} and only

limited information is available for carbonate reservoirs: Roustaei and Bagherzadeh⁴² conducted coreflood tests and they demonstrated that nanofluid-EOR can increase oil production by 9-17% depending on ageing time, and Zhang, et al.⁴⁰ have investigated the adsorption behaviour of silica nanoparticles on calcite powder.

We thus examine the wettability alteration efficiency of silica nanofluids on oil-wet and intermediate-wet calcite surfaces and how various factors influence this efficiency. All experiments were conducted at ambient conditions. At reservoir conditions, however, significantly higher pressures and elevated temperatures prevail, and as pressure and particularly temperature can affect nanofluid properties²⁸, nanofluid efficiency at reservoir conditions may be different to that measured at ambient conditions; furthermore, nanofluid efficiency is probably also influenced by rock heterogeneity, which determines nanofluid flow and distribution^{5, 43} throughout the formation.

2. Experimental Methodology

2.1 Materials

N-decane (> 99mol %, from Sigma-Aldrich) was used as a model oil. N-hexane (> 95mol %, from Sigma-Aldrich), nitrogen (> 99.99mol%, from BOC), acetone and methanol (> 99.9mol%, from Rowe Scientific) were used as cleaning agents. Deionized (DI) water (Ultrapure from David Gray; conductivity = 0.02 mS/cm) and sodium chloride (≥ 99.5 mol%, from Scharlan) were used to prepare brines (0-20 wt% NaCl).

Silicon dioxide nano-powder (porous spheres, Sigma Aldrich) was used to prepare the nanofluids (general properties are listed in Table 1).

Table 1: Properties of silicon dioxide nanoparticles (Sigma Aldrich 2015).

Particle size [nm]	5-15
Purity [wt%]	99.5
Density [kg/m ³]	(2200-2600)
Boiling point [K]	2503
Melting point [K]	1873

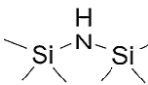
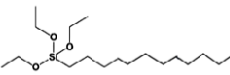
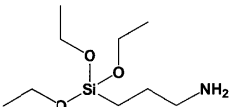
Molecular mass [g/mol]	60.08
Solubility in water	Insoluble

Iceland spar samples (pure calcite, from WARD'S Natural Science) were used as substrates; the surface topography of the calcite samples was measured with an atomic force microscope (model DSE 95-200), Figure 4, as surface roughness influences wettability⁴⁴ and adsorption rate of nanoparticles.⁴⁵ Prior to nano-treatment, all calcite samples were very smooth with root mean square (RMS) surface roughness between 18-32 nm.

Pure calcite, however, is strongly water-wet.^{14,46} This was confirmed by our contact angle measurements on clean substrates (the water contact angle θ was 0°). We note that in the literature slightly higher contact angles were reported, probably due to insufficient cleaning.⁴⁷ Consequently, it was necessary to render the calcite surface oil-wet to simulate an oil (or CO₂ storage) reservoir. To accomplish this, the calcite surfaces were treated with a range of silanes:^{48,49} hexamethyldisilazane (HMDS), dodecyltriethoxysilane and (3-aminopropyl) triethoxysilane (Table 2). We note that previously some researchers used naphthenic acids or crude oil for wettability alteration, however, such a wettability change is unstable and leads to only weakly water-wet or intermediate-wet surfaces¹⁴, rather than clearly oil-wet surfaces.

Table 2: Silanes used and their properties (Sigma Aldrich 2015).

Silane	Chemical Formula	Chemical Structure	Molecular mass [g/mol]	Boiling point [K]	Density [kg/m ³]

Hexamethyldisilazane	$(\text{CH}_3)_3\text{SiNHSi}(\text{CH}_3)_3$		161.39	398	770
Dodecyltriethoxysilane	$\text{C}_{18}\text{H}_{40}\text{O}_3\text{Si}$		332.59	538.4	875
(3-aminopropyl) triethoxysilane	$\text{H}_2\text{N}(\text{CH}_2)_3\text{Si}(\text{OC}_2\text{H}_5)_3$		221.37	490	946

2.2 Calcite surface preparation

The calcite surfaces were flushed with DI water and rinsed with toluene to remove any organic contaminants. Subsequently, the samples were dried for 10 min at 40 °C and exposed to air plasma^{47, 50} for 40 min to remove any residual contaminants. It is important to properly clean the samples' surfaces as residual contaminations can lead to dramatic systematic errors.^{47, 51, 52} Silanization started directly after surface preparation to minimize any contamination.

Surface modification with silanes

Three different silanes were used to render the calcite surfaces to oil wet (Table 2). Each cleaned calcite substrate was placed in a separate small glass bottle and silane was pipetted gradually over the sample surface until the substrate was fully immersed in silane. The bottle was then tightly sealed to prevent any evaporation or sample contamination. Subsequently, the bottles were placed in an oven and heated at 363 K for 24 h. Finally, the calcite surfaces were washed with n-hexane and methanol in order to remove excess silane and finally flushed with DI water before drying with pure nitrogen. During this process the silyl groups of the silane reacted with the hydroxyl groups on the surface forming siloxane bonds (Figure 1; London, et al.⁵³). As a result, alkyl (or aminoalkyl) groups were chemically bonded to the surface, which rendered the surface more oil-wet. The alkyl groups are more representative of lighter oil, while the amino-alkyl, with its heteroatom nitrogen, mimics more medium density oil with significant resin contents.⁵⁴ We quantified the degree of wettability alteration by dispensing a drop of water onto the surfaces in air or n-decane (Table 3) using the tilted plate method,⁵⁵ see below.

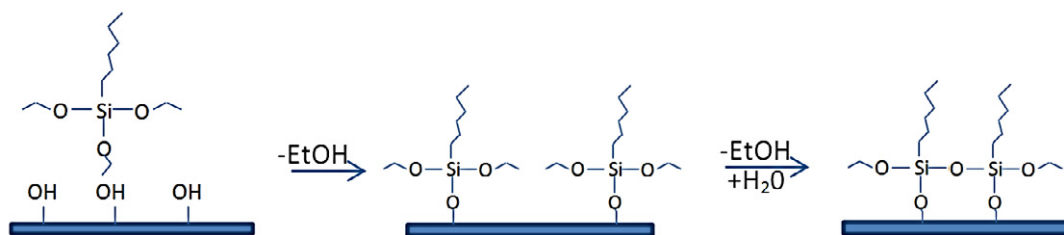


Figure 1: Silylation of calcite surface⁵⁶ (after London, et al.⁵³).

Hexamethyldisilazane and dodecyltriethoxysilane were very effective in terms of increasing the water contact angle θ . Water advancing contact angles θ_a (which are relevant for the water imbibition process into the small rock capillaries) reached ~ 130 - 140° . The 3-aminopropyltriethoxysilane was less effective, and mixed-wet substrates were obtained ($\theta \sim 70^\circ$), probably due to the higher polarity of the terminal amine group. We note that the measured water contact angles were significantly higher in n-decane than in air, and we conclude that tests should be conducted with oil as this is more relevant. As dodecyltriethoxysilane altered the surface to the most oil-wet state, we selected this silane for all subsequent studies.

Table 3: Water contact angles on silane-modified calcite surfaces (ambient conditions).

Silane	n-decane		air	
	advancing	receding	advancing	receding
	θ_a [°]	θ_r [°]	θ_a [°]	θ_r [°]
Hexamethyldisilazane	129	120	76	71
Dodecyltriethoxysilane	141	129	93	88
(3-aminopropyl) triethoxysilane	73	66	47	39

2.3 Nanofluid Preparation

Various nanofluids were tested for their ability to render oil-wet calcite surfaces water-wet. These fluids were formulated by homogenizing the silicon dioxide nanoparticles (properties are listed in Table 1) in brine with an ultrasonic homogenizer (300 VT Ultrasonic Homogenizer/ BIOLOGICS) for 120 min¹⁸. We note that magnetic stirring is insufficient to homogenize such fluids.⁵⁷ Specifically, a titanium micro tip with a 9.5mm diameter was used to prepare 100 mL batches of nanofluid using a sonication power of 240W. Each batch was sonicated for 8 periods of 15 minutes with 5 minutes rest to avoid overheating. After sonication, the nanofluid was stored in a dark and cool environment for 2 hours to ensure stability and homogeneity. Different nanoparticle concentrations (0.5- 4wt%) and brine salinities (0-20wt% NaCl) were tested; nanofluid and brine densities were measured at room conditions (Figure 2) with an Anton Paar DMA 4500 densitometer (accuracy ± 0.0001 g/cm³).

The phase behaviour of the nanofluids was monitored by taking photos of the test tubes every 30 min in the first 6 hours and every 6 hours over 6 weeks. During this time all nanofluids with SiO₂ concentrations above 0.5wt% showed stable behaviour. At lower nanoparticle concentration, however, and especially at high salinities (≥ 15 wt%), instabilities (i.e. nanoparticle flocculation within hours) were observed; this is related to the screening effect of electrolytes on the electrostatic repulsion forces between the nanoparticles: high electrolyte concentration reduces this repulsive forces,⁵⁸ which leads to accelerated coalescence and sedimentation of nanoparticles after homogenization, particularly at low nanoparticle concentration.

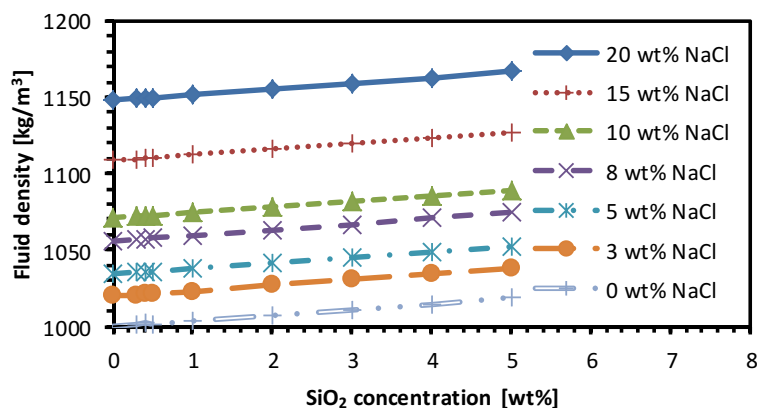


Figure 2: Densities of various nanofluids used.

2.4 Surface modification with nanofluid (Nano-modification) and Contact angle measurements

In order to test the efficiency of the nanofluids in terms of wettability alteration, the oil-wet calcite substrates were immersed in the nanofluid at room conditions for prescribed exposure times (1-100 h). Subsequently, contact angles were again measured.

Specifically, advancing and receding water contact angles were measured using the tilted plate technique.⁵⁵ Generally, 6-7 μ L water drops were dispensed onto the substrate,⁴⁵ which was placed on a metal platform at an inclination angle of 17°. The water contact angles were measured just before the drop started to move following the procedure described by Al-Yaseri et al. (2015)⁵⁹ The whole process was recorded with a high resolution video camera (Basler scA 640–70 fm, pixel size = 7.4 μ m; frame rate = 71 fps; Fujinon CCTV lens: HF35HA-1B; 1:1.6/35 mm) and θ was measured on images extracted from these movies with Image J software. The standard deviation for the θ measurements was $\pm 3^\circ$ based on replicate measurements. The water advancing contact angle is associated with the imbibing water front in a reservoir or individual capillary, and θ_a is thus most important for the applications described in this study. We note that θ_a is a key variable in pore-scale fluid dynamics models,^{60, 61} with which oil production curves or CO₂ spreading behaviour in rock can be calculated.

3. Results and discussion

A shift in rock surface wettability from oil-wet to water-wet is expected to significantly increase oil production particularly from fractured formations where spontaneous imbibition of water is the prime production mechanism.^{14,26} Furthermore, significantly higher CO₂ trapping capacities have been predicted for carbon geo-storage projects, if the rock is strongly water-wet.^{30,31} This is true for the structural trapping capacity, where a lower water contact angle raises the capillary entry pressure of the caprock, and thus significantly increases the column height of CO₂, which can be permanently immobilized beneath the caprock³¹. And it is also true for the capillary trapping capacity of CO₂⁶², where lower water contact angles lead to more frequent snap-off and trapping of CO₂ bubbles (which are trapped in the pore network of the rock matrix by capillary forces; cp. Iglauer et al. 2011³⁵ versus Chaudhary et al. 2013³⁶, and Pentland et al. 2011³³). Here we discuss how application of nanofluids can achieve a substantial wettability change, and the effect of different parameters on this change.

3.1 SEM-EDS and AFM analysis

Surface modification was probed with a scanning electron microscope (SEM, Zeiss Neon 40EsB FIBSEM) and energy dispersive x-ray spectroscopy (EDS, Oxford X-act SSD x-ray detector with Inca and Aztec software). Significant silicon concentrations were detected on five points on the sample surface after nano-modification (Table 4), which indicates that nanoparticles were rather homogeneously distributed on the surface, consistent with previous studies on glass and silicon substrates.^{7,63} The slight variation of silica concentration is related to small perturbations in the nanofluid's homogeneity and the surface roughness of the substrate.^{40, 64}

Table 4: Surface composition of the oil-wet calcite substrates after modification with nanofluid (2wt% SiO₂ in 20wt% NaCl brine, 12 hours exposure time).

Point	Calcium [wt%]	Silicon [wt%]	Oxygen wt%
1	33.4	1.9	64.7
2	35.2	2.3	62.5
3	32.6	3.3	64.1
4	33.4	1.9	64.7
5	35.2	2.3	62.5

The SEM images revealed significant adsorption of nanoparticles onto the calcite surface; and these adsorbed particles partially agglomerated into larger clusters (Figure 3). While the original calcite surface was very flat (except a crystal layer edge), exposure to nanofluid changed the surface morphology significantly, and an irregularly spreaded coating was visible. On all SEM images the irreversibly adsorbed fraction was imaged (i.e. the substrate was exposed to different cleaning fluids, see section 3.3).

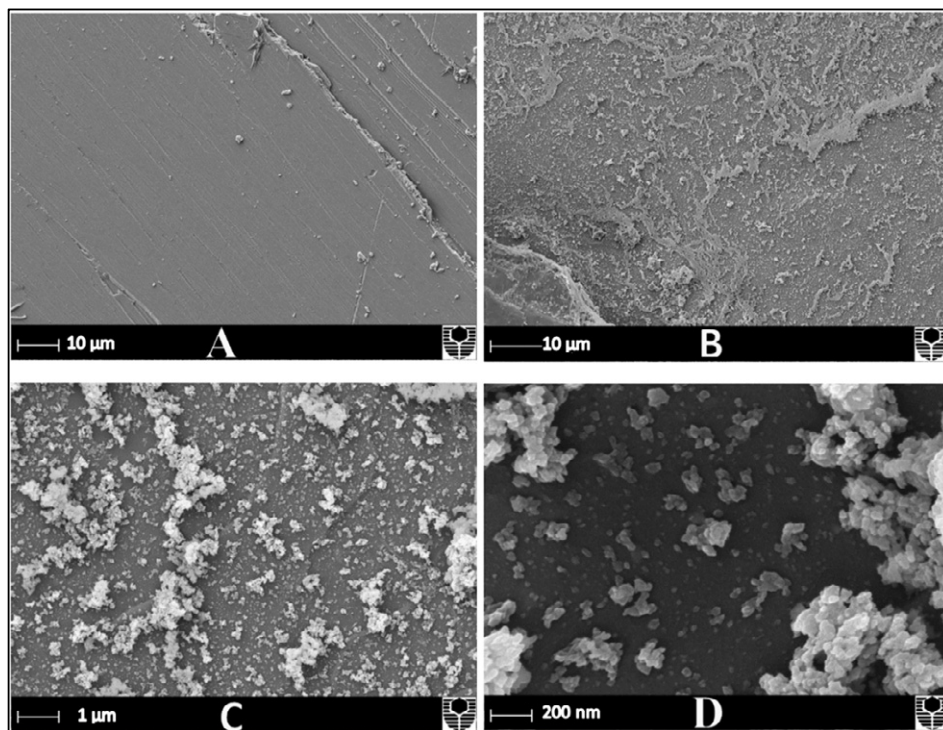


Figure 3: SEM images of an oil-wet calcite surface: a) before; b) after nanofluid treatment (4wt% SiO₂ in 5wt% NaCl brine, 1 hour exposure time); c) high resolution; and d) maximum resolution zoom-into the irreversibly adsorbed silica nanoparticles.

These results are consistent with AFM measurements performed on the nano-treated calcite substrates (Figure 4): Higher surface roughness was found on the nano-treated surface: the RMS surface roughness increased to 350-3000nm (from 18-32nm) and associated z-ranges (i.e. peak heights) increased to 550-5000nm (from 30-300nm). The AFM images also confirmed quasi-homogeneous spread of the adsorbed nanoparticles on the surface.

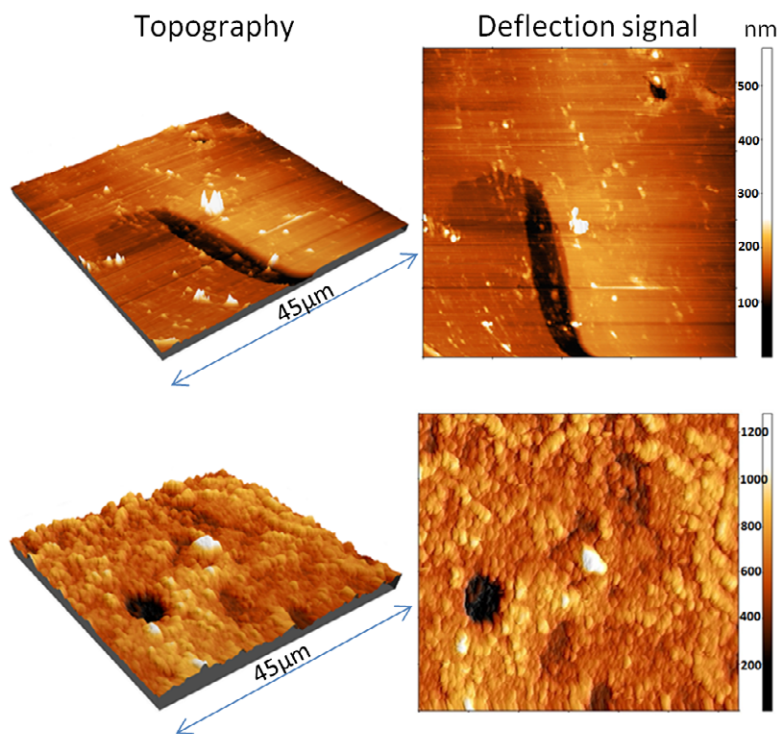


Figure 4: Atomic force microscopy images of a calcite surface used in the experiments before (upper image) and after (lower image) nano-modification. The RMS surface roughness before nano-modification was 32 nm, which is very smooth. After nanofluid treatment (0.5wt% SiO₂ in 10wt% NaCl brine for 4 hr) the RMS surface roughness increased to 1300 nm. Different colours refer to variations in height (black: 0nm, white: peak height = 640nm [upper image], 1300 nm [lower image]).

3.2 Effect of exposure time on contact angle

As the surface modification is caused by nanoparticle adsorption (see above), longer contact time leads to decreased θ (through increased adsorption), Figure 5 (θ in air decreased from 77° to 18° after 1 h and to 10° after 3 h exposure time; and θ in n-decane decreased from 122° to 30° after 1 h and further to 18° after 3 h exposure time). θ rapidly decreased within the first 60 minutes of exposure followed by further, but smaller, reduction in θ (Figure 5). After 3h exposure time no further change in θ was observed. We conclude that the sample reached adsorption capacity after three hours. This is consistent with the trend observed by Roustaei and Bagherzadeh⁴² on limestone and Zhang, et al.,⁴⁰ who demonstrated that a smaller flow

rate of nanofluid through a calcite powder increased nano-silica adsorption (since contact time increased).

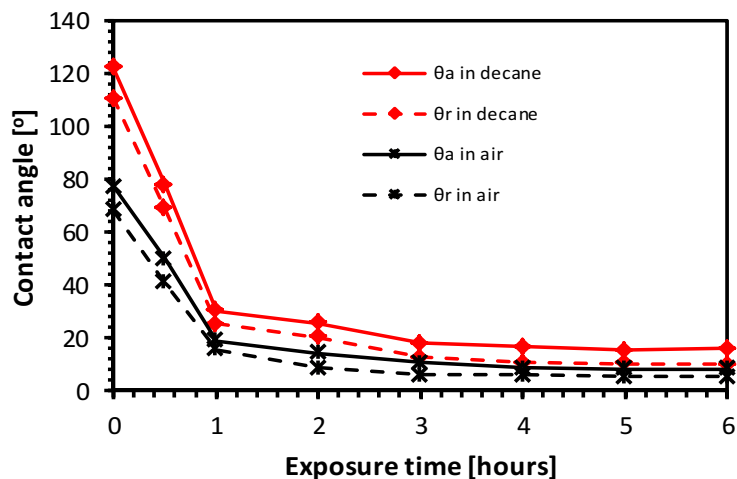


Figure 5: Water contact angles on oil-wet calcite surface in air and n-decane as a function of exposure time to nanofluid (2wt% SiO₂, 5wt% NaCl brine).

3.3 Adsorption characteristics: reversible versus irreversible adsorption

Adsorption characteristics related to nanofluid surface modification were further studied as this fundamentally influences the success of the application. Of particular interest is the ratio between reversibly and irreversibly bonded silica, and thus the stability of nanofluid modification. We therefore exposed the nano-modified calcite surface to various solvents:

- 1- Oil-wet calcite surface [not nano-modified]
- 2- Nanofluid
- 3- Nanofluid and DI water
- 4- Nanofluid, acetone, and DI water
- 5- Procedure 4 followed by second rinsing with acetone and DI water

After each step, the substrate was dried with N₂ gas, and the advancing and receding contact angles were measured (Figure 6).

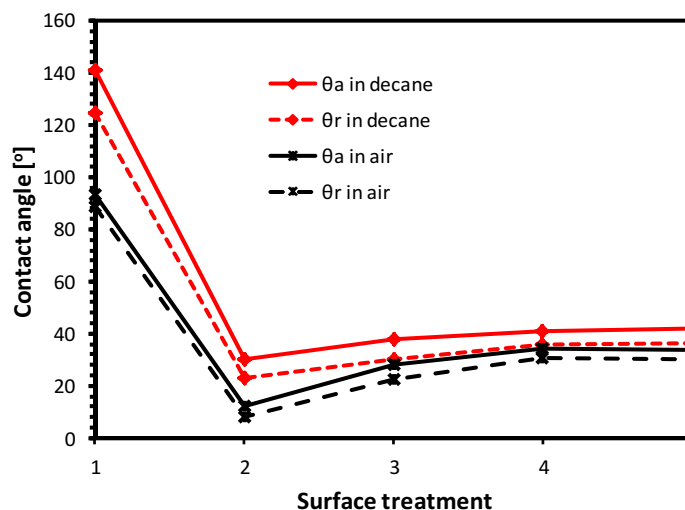


Figure 6: Water contact angles on: 1) oil-wet calcite surface in air and n-decane; 2) after nano-modification (2wt% SiO₂, 20wt% NaCl brine, 1 hour exposure time); 3) DI water; 4) acetone; 5) 2nd acetone and water rinse.

Most nanoparticles were bonded irreversibly, which is in agreement with observations for sandstone surfaces.²⁶ Quantitatively, the total difference in contact angle after removal of the reversibly bonded nanoparticles was $\sim 15^\circ$, which is smaller than the drastic reduction caused by the nanofluid itself (-98°). Mechanistically, it is likely that the silica nanoparticles chemisorbed onto the surface (on patches which were not modified by the silane and thus contained surface silanol groups⁶⁵; such silanol groups probably strongly interacted with the silanol groups on the silica particle surface, this has also been observed in recent formation damage studies, Al-Yaseri et al. 2015⁶⁶). These adsorption effects were observed with AFM and on SEM images, see above.

3.4 Effect of electrolyte concentration on contact angle

It is well known that the electrolyte concentration significantly influences nanofluid properties;^{7,58} and at the same time it is well established that the salinity of formation brine can vary greatly and can reach very high levels.³⁴ It is thus necessary to investigate the effect of salinity on θ and nanofluid stability.

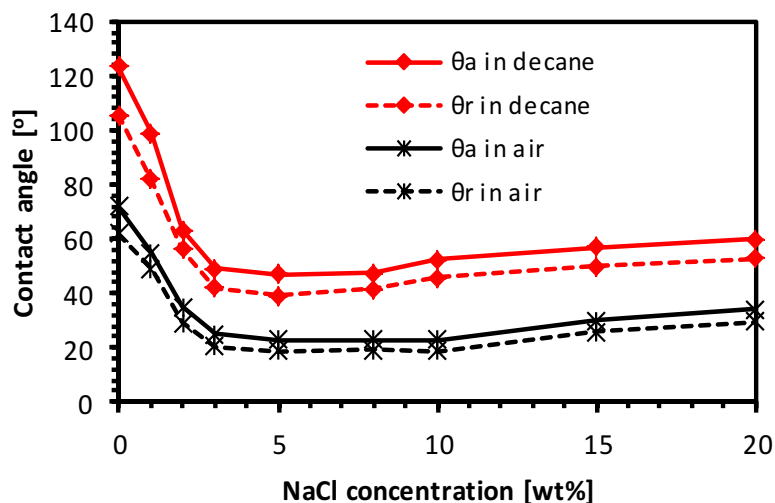


Figure 7: Water contact angles on nano-modified calcite surface in air and n-decane as a function of brine salinity (2wt% SiO₂, 1 hour exposure time).

We therefore systematically measured θ as a function of NaCl concentration; θ was high for DI water (100-125° for n-decane), and much lower for all tested brines (40-50° in n-decane), Figure 7. θ reached a minimum at 3wt% NaCl concentration, which implies that there is an optimum salinity similar to that found in surfactant formulations.^{67, 68} In case of the 2wt% SiO₂ nanofluid, optimal NaCl concentrations ranged between 3-8 wt% (Figure 7). Salinity thus plays a crucial role in wettability alteration by nanofluid. Nanofluid treatment had a significant effect on the contact angle in DI water (θ reduction by 17.5°), but this effect was massively enhanced when electrolytes were present (reduction of θ by 95° in case of 3wt% NaCl brine).

This behaviour is related to the stability of the dispersed nanoparticles, which is controlled by their surface charge (note that the zeta potential for silica nanoparticles is around -45 mV for the pH range 6-10; Metin, et al.⁶⁹). This negative surface charge creates electrostatic repulsion forces, which prevent nanoparticle agglomeration²⁴ and sedimentation. Electrolytes weaken the net repulsion forces between the nanoparticles and thus accelerate the precipitation of nanoparticles onto the calcite surface.⁵⁸ As a consequence, increasing nanofluid salinity increases wettability alteration efficiency. However, at high salinities (>10

wt% NaCl) the repulsion forces are dramatically reduced²⁴, which increases the rate of agglomeration between these particles⁷ and slightly reduces efficiency (Figure 7).

3.5 Effect of nanoparticle concentration in nanofluid

While higher nanoparticle concentrations are expected to be more efficient (i.e. reduce θ more and faster, Roustaei and Bagherzadeh⁴²), it is vital from an economical perspective that costs are minimized, and typically only small amounts of additives are profitable (e.g. Iglauer, et al.^{35,68,70}). Thus, it is necessary to determine the smallest effective nanoparticle concentration. Furthermore, high concentrations of nanoparticles (>3 wt%) may reduce reservoir permeability,⁵ which should be avoided. In this study we found that nanoparticle concentration at 1 wt% changed the oil-wet surface (initially $\theta = 120^\circ$) into a weakly water-wet state ($\theta = 60^\circ$), and into a strongly water-wet state at 2wt% nanoparticle concentration ($\theta = 45^\circ$, versus n-decane, Figures 8).

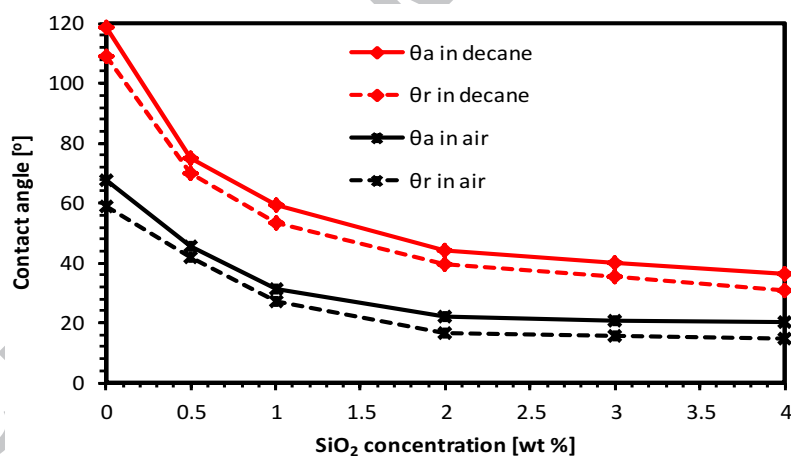


Figure 8: Water contact angles on nano-modified calcite surface in air and n-decane as a function of SiO₂ concentration in the nanofluid (10 wt %NaCl, 1 hour exposure time).

Moreover, a threshold value ($\sim 2\text{wt}\%$ silica concentration) was observed, above which θ did not change, consistent with data reported for silicon (Munshi, et al.⁴⁵) and glass (Nikolov, et al.⁶³).

3.6 Nanofluid-rock re-equilibration processes

Here we tested whether repeated nanofluid usage changes its effectiveness. Such a scenario with constantly re-equilibrating fluid-rock interactions simulates the leading edge of the nanofluid flood in the formation, and associated adsorption-desorption-transport phenomena need to be considered. No significant differences in contact angle were observed for fresh versus used nanofluid (Figure 9), consistent with previous studies reported for powdered calcite.⁴⁰

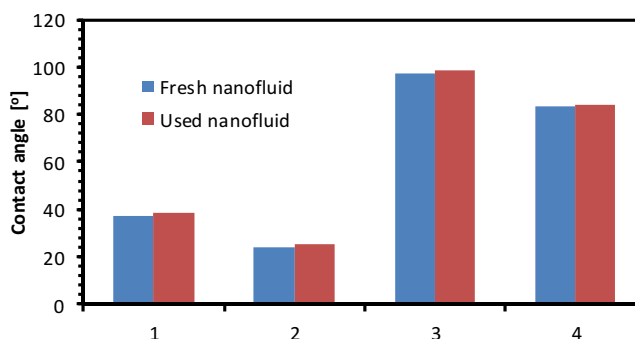


Figure 9: Differences in water contact angle between fresh and used nanofluid (0.5wt % SiO_2 , 20 wt% NaCl, and 1 hour exposure time): 1) θ_a in air, 2) θ_r in air, 3) θ_a in n-decane, 4) θ_r in n-decane.

4. Conclusions

Hydrocarbon production from fractured, oil-wet limestone reservoirs is a big challenge as conventional recovery techniques are inefficient,^{71,72} mainly due to water not spontaneously imbibing into the oil-wet rock matrix. Production would, however, be dramatically increased, if the rock matrix could be rendered water-wet (so that water can spontaneously imbibe and displace oil¹⁴). Furthermore, it is highly desirable to change oil-wet surfaces more water-wet

in carbon geo-sequestration projects to increase storage capacities and de-risk containment security^{30, 73}. Despite the vital importance for limestone reservoirs, previous studies focused on sandstone formations,^{21,25,26,28,41} and only limited information is available for carbonate reservoirs.^{40, 42}

It is therefore now necessary to better understand the fundamental characteristics of nanofluid-carbonate interactions and how wettability is affected; thus we investigated the wettability alteration efficiency of various nanofluids on oil-wet carbonate.

Tested parameters included nanoparticle concentration, nanofluid salinity, surface modification time, and reversibility of nanoparticle adsorption as these variables have been previously shown to affect nanofluid treatment performance.^{24,26,40, 42}

We found that nanofluids can change the wettability of oil-wet calcite to strongly water-wet under condition. Exposure time played a major role, and after ~1 hour, most of the wettability change was achieved, consistent with the results of Roustaei and Bagherzadeh.⁴⁰ It was furthermore observed that nanoparticle adsorption was mainly irreversible, although a partially reversible behaviour was measured after washing the surface with acetone and/or DI water. The minimum effective nanoparticle concentration was 1-2wt%, consistent with data reported for clay (Shamsijazeyi, et al.⁵). Moreover, an optimum salinity range was detected (3-8wt % NaCl concentration), similar to the optimum salinity in surfactant formulations.^{67, 68}

We note that pressure and particularly temperature can significantly affect nanofluid properties²⁸, thus nanofluid behaviour and efficiency at reservoir conditions may be different; furthermore nanofluid efficiency is also likely affected by rock heterogeneity, which influences nanoparticle transport within the solid matrix⁴³.

Technically, nanofluid would be injected through the wellbore and hydraulically pressed into the fractures. From there the particles diffuse into the pore matrix⁷⁴ or they are pumped deeper into the formation by the viscous pressure gradient.

Overall, we conclude that nanofluids can be very efficient in terms of wettability alteration. Thus such formulations have a high potential in the area of enhanced oil production or CO₂ geo-storage.

Acknowledgements

Sarmad Al-Anssari would like to thank the Iraqi Federal Government for PhD scholarship.

References

- (1) Lohse, S. E.; Murphy, C. J. Applications of Colloidal Inorganic Nanoparticles: From Medicine to Energy. *Journal of the American Chemical Society* **2012**, *134* (38), 15607-15620.
- (2) Tong, R.; Hemmati, H. D.; Langer, R.; Kohane, D. S. Photoswitchable Nanoparticles for Triggered Tissue Penetration and Drug Delivery. *Journal of the American Chemical Society* **2012**, *134* (21), 8848-8855.
- (3) De, M.; Ghosh, P. S.; Rotello, V. M. Applications of Nanoparticles in Biology. *Advanced Materials* **2008**, *20* (22), 4225-4241.
- (4) Rajauria, S.; Axline, C.; Gottstein, C.; Cleland, A. N. High-Speed Discrimination and Sorting of Submicron Particles Using a Microfluidic Device. *Nano Letters* **2015**, *15* (1), 469-475.
- (5) ShamsiJazeyi, H.; Miller, C. A.; Wong, M. S.; Tour, J. M.; Verduzco, R. Polymer-coated nanoparticles for enhanced oil recovery. *Journal of Applied Polymer Science* **2014**, *131* (15), 1-13.
- (6) Wang, H.; Yan, N.; Li, Y.; Zhou, X.; Chen, J.; Yu, B.; Gong, M.; Chen, Q. Fe nanoparticle-functionalized multi-walled carbon nanotubes: one-pot synthesis and their applications in magnetic removal of heavy metal ions. *Journal of Materials Chemistry* **2012**, *22* (18), 9230-9236.
- (7) Winkler, K.; Paszewski, M.; Kalwarczyk, T.; Kalwarczyk, E.; Wojciechowski, T.; Gorecka, E.; Pocięcha, D.; Holyst, R.; Fialkowski, M. Ionic Strength-Controlled Deposition of Charged Nanoparticles on a Solid Substrate. *The Journal of Physical Chemistry C* **2011**, *115* (39), 19096-19103.
- (8) Balaji, T.; Yulia, B.; Atikur, R.; Saiful, I.; Mizanur, R.; Azharul, I.; Joslyn, P.; James, K.; Jasmine, T.; Dhananjay, K.; Shamsuddin, I.; Debasish, K. Development of Mesoporous Silica Encapsulated Pd-Ni Nanocatalyst for Hydrogen Production. In *Production and Purification of Ultraclean Transportation Fuels*; American Chemical Society, **2011**, 1088, 177-190.
- (9) Wilson, G. J.; Matijasevich, A. S.; Mitchell, D. R. G.; Schulz, J. C.; Will, G. D. Modification of TiO₂ for Enhanced Surface Properties: Finite Ostwald Ripening by a Microwave Hydrothermal Process. *Langmuir* **2006**, *22* (5), 2016-2027.
- (10) Zhang, H.; Nikolov, A.; Wasan, D. Enhanced Oil Recovery (EOR) Using Nanoparticle Dispersions: Underlying Mechanism and Imbibition Experiments. *Energy & Fuels* **2014**, *28* (5), 3002-3009.
- (11) Sharma, G.; Mohanty, K. Wettability Alteration in High-Temperature and High-Salinity Carbonate Reservoirs. *SPE Journal* **2013**, *18* (4), 646-655.
- (12) Gupta, R.; Mohanty, K. Temperature Effects on Surfactant-Aided Imbibition Into Fractured Carbonates. *SPE Journal* **2010**, *25* (1), 80-88.
- (13) Mason, G.; Morrow, N. R. Developments in spontaneous imbibition and possibilities for future work. *Journal of Petroleum Science and Engineering* **2013**, *110* (0), 268-293.

- (14) Wu, Y.; Shuler, P. J.; Blanco, M.; Tang, Y.; Goddard, W. A. An Experimental Study of Wetting Behavior and Surfactant EOR in Carbonates with Model Compounds. *SPE Journal* **2008**, *13* (1), 26-34.
- (15) Rostami Ravari, R.; Strand, S.; Austad, T. Combined Surfactant-Enhanced Gravity Drainage (SEGD) of Oil and the Wettability Alteration in Carbonates: The Effect of Rock Permeability and Interfacial Tension (IFT). *Energy & Fuels* **2011**, *25* (5), 2083-2088.
- (16) Ding, B.; Zhang, G.; Ge, J.; Liu, X. Research on Mechanisms of Alkaline Flooding for Heavy Oil. *Energy & Fuels* **2010**, *24* (12), 6346-6352.
- (17) Guo, Z.; Dong, M.; Chen, Z.; Yao, J. Dominant Scaling Groups of Polymer Flooding for Enhanced Heavy Oil Recovery. *Industrial & Engineering Chemistry Research* **2013**, *52* (2), 911-921.
- (18) Shen, M.; Resasco, D. E. Emulsions Stabilized by Carbon Nanotube–Silica Nanohybrids. *Langmuir* **2009**, *25* (18), 10843-10851.
- (19) Al-Manasir, N.; Kjøniksen, A.-L.; Nyström, B. Preparation and characterization of cross-linked polymeric nanoparticles for enhanced oil recovery applications. *Journal of Applied Polymer Science* **2009**, *113* (3), 1916-1924.
- (20) Cui, Z. G.; Yang, L. L.; Cui, Y. Z.; Binks, B. P. Effects of Surfactant Structure on the Phase Inversion of Emulsions Stabilized by Mixtures of Silica Nanoparticles and Cationic Surfactant. *Langmuir* **2009**, *26* (7), 4717-4724.
- (21) Sharma, T.; Suresh Kumar, G.; Sangwai, J. S. Enhanced oil recovery using oil-in-water (o/w) emulsion stabilized by nanoparticle, surfactant and polymer in the presence of NaCl. *Geosystem Engineering* **2014**, *17* (3), 195-205.
- (22) Zargartalebi, M.; Barati, N.; Kharrat, R. Influences of hydrophilic and hydrophobic silica nanoparticles on anionic surfactant properties: Interfacial and adsorption behaviors. *Journal of Petroleum Science and Engineering* **2014**, *119* (0), 36-43.
- (23) Zhu, D.; Han, Y.; Zhang, J.; Li, X.; Feng, Y. Enhancing rheological properties of hydrophobically associative polyacrylamide aqueous solutions by hybridizing with silica nanoparticles. *Journal of Applied Polymer Science* **2014**, *131* (19), 1-8.
- (24) Zargartalebi, M.; Kharrat, R.; Barati, N. Enhancement of surfactant flooding performance by the use of silica nanoparticles. *Fuel* **2015**, *143* (0), 21-27.
- (25) Ju, B.; Fan, T.; Ma, M. Enhanced oil recovery by flooding with hydrophilic nanoparticles. *China Particuology* **2006**, *4* (1), 41-46.
- (26) Ju, B.; Fan, T. Experimental study and mathematical model of nanoparticle transport in porous media. *Powder Technology* **2009**, *192* (2), 195-202.
- (27) Suleimanov, B. A.; Ismailov, F. S.; Veliyev, E. F. Nanofluid for enhanced oil recovery. *Journal of Petroleum Science and Engineering* **2011**, *78* (2), 431-437.
- (28) Hendraningrat, L.; Li, S.; Torsæter, O. A coreflood investigation of nanofluid enhanced oil recovery. *Journal of Petroleum Science and Engineering* **2013**, *111* (0), 128-138.
- (29) Maerker, J.M., and Gale, W.W. Surfactant flood process design for Loudon. *SPE Journal* **1992**.7(1):36-44
- (30) Iglauer, S.; Pentland, C. H.; Busch, A. CO₂ wettability of seal and reservoir rocks and the implications for carbon geo-sequestration. *Water Resources Research* **2015**, *51* (1), 729-774.
- (31) Iglauer, S.; Al_Yaseri, A.Z.; Rezaee, R., and M. Lebedev. CO₂-wettability of caprocks: implications for storage capacity and containment security. *Geophysical Research Letters* **2015**, in press.

- (32) Spiteri, E. J., Juanes, R., Blunt, M. J., & Orr, F. M. A New Model of Trapping and Relative Permeability Hysteresis for All Wettability Characteristics. *SPE Journal* **2008**, 13 (03), 277-288
- (33) Pentland, Christopher and El-Maghraby, Rehab and Iglauer, Stefan and Blunt, Martin. Measurements of the capillary trapping of super-critical carbon dioxide in Berea sandstone. *Geophys. Res. Lett* **2011**, 38 (L06401).
- (34) Iglauer, S.; Mathew, M. S.; Bresme, F. Molecular dynamics computations of brine–CO₂ interfacial tensions and brine–CO₂–quartz contact angles and their effects on structural and residual trapping mechanisms in carbon geo-sequestration. *Journal of Colloid and Interface Science* **2012**, 386 (1), 405-414.
- (35) Iglauer, S.; Paluszny, A.; Pentland, C. H.; Blunt, M. J. Residual CO₂ imaged with X-ray micro-tomography. *Geophys. Res. Lett* **2011**, 38 (21), 1-6
- (36) Chaudhary, K., M. Bayani Cardenas, W.W Wolf, J. A. Ketcham, and P. C. Bennett, Pore-scale trapping of supercritical CO₂ and the role of grain wettability and shape, *Geophys. Res. Lett.* **2013**, 40, 3878-3882
- (37) Mahbubul, I. M.; Chong, T. H.; Khaleduzzaman, S. S.; Shahrul, I. M.; Saidur, R.; Long, B. D.; Amalina, M. A. Effect of Ultrasonication Duration on Colloidal Structure and Viscosity of Alumina–Water Nanofluid. *Industrial & Engineering Chemistry Research* **2014**, 53 (16), 6677-6684.
- (38) Arns, C. H.; Bauget, F.; Limaye, A.; Sakellariou, A.; Senden, T.; Sheppard, A.; Sok, R. M.; Pinczewski, V.; Bakke, S.; Berge, L. I.; Oren, P. E.; Knackstedt, M. A. Pore Scale Characterization of Carbonates Using X-Ray Microtomography. *SPE Journal* **2005**, 10 (4), 475-484.
- (39) Petosa, A. R.; Jaisi, D. P.; Quevedo, I. R.; Elimelech, M.; Tufenkji, N. Aggregation and Deposition of Engineered Nanomaterials in Aquatic Environments: Role of Physicochemical Interactions. *Environmental Science & Technology* **2010**, 44 (17), 6532-6549.
- (40) Zhang, T.; Murphy, M. J.; Yu, H.; Bagaria, H. G.; Yoon, K. Y.; Nielson, B. M.; Bielawski, C. W.; Johnston, K. P.; Huh, C.; Bryant, S. L. Investigation of Nanoparticle Adsorption During Transport in Porous Media. *SPE Journal* **2014**, preprint, 1-11.
- (41) Maghzi, A.; Mohebbi, A.; Kharrat, R.; Ghazanfari, M. Pore-Scale Monitoring of Wettability Alteration by Silica Nanoparticles During Polymer Flooding to Heavy Oil in a Five-Spot Glass Micromodel. *Transp Porous Med* **2011**, 87 (3), 653-664.
- (42) Roustaei, A.; Bagherzadeh, H. Experimental investigation of SiO₂ nanoparticles on enhanced oil recovery of carbonate reservoirs. *J Petrol Explor Prod Technol* **2014**, 1-7.
- (43) Skaug, M. J., Wang, L., Ding, Y., & Schwartz, D. K. Hindered Nanoparticle Diffusion and Void Accessibility in a Three-Dimensional Porous Medium. *ACS Nano* **2015**, 9(2), 2148-2156.
- (44) Marmur, A. Soft contact: measurement and interpretation of contact angles. *Soft Matter* **2006**, 2 (1), 12-17.
- (45) Munshi, A. M.; Singh, V. N.; Kumar, M.; Singh, J. P. Effect of nanoparticle size on sessile droplet contact angle. *Journal of Applied Physics* **2008**, 103 (8), 1-5.
- (46) Espinoza, D. N.; Santamarina, J. C. Water-CO₂-mineral systems: Interfacial tension, contact angle, and diffusion--Implications to CO₂ geological storage. *Water Resources Research* **2010**, 46 (7), 1-15.

- (47) Iglauer, S.; Salamah, A.; Sarmadivaleh, M.; Liu, K.; Phan, C. Contamination of silica surfaces: Impact on water–CO₂–quartz and glass contact angle measurements. *International Journal of Greenhouse Gas Control* **2014**, *22* (0), 325-328.
- (48) Kallury, K. M. R.; Macdonald, P. M.; Thompson, M. Effect of Surface Water and Base Catalysis on the Silanization of Silica by (Aminopropyl)alkoxysilanes Studied by X-ray Photoelectron Spectroscopy and ¹³C Cross-Polarization/Magic Angle Spinning Nuclear Magnetic Resonance. *Langmuir* **1994**, *10* (2), 492-499.
- (49) Grate, J. W.; Dehoff, K. J.; Warner, M. G.; Pittman, J. W.; Wietsma, T. W.; Zhang, C.; Oostrom, M. Correlation of Oil–Water and Air–Water Contact Angles of Diverse Silanized Surfaces and Relationship to Fluid Interfacial Tensions. *Langmuir* **2012**, *28* (18), 7182-7188.
- (50) Sarmadivaleh, M.; Al-Yaseri, A. Z.; Iglauer, S. Influence of temperature and pressure on quartz–water–CO₂ contact angle and CO₂–water interfacial tension. *Journal of Colloid and Interface Science* **2015**, *441* (0), 59-64.
- (51) Love, J. C.; Estroff, L. A.; Kriebel, J. K.; Nuzzo, R. G.; Whitesides, G. M. Self-Assembled Monolayers of Thiolates on Metals as a Form of Nanotechnology. *Chemical Reviews* **2005**, *105* (4), 1103-1170.
- (52) Mahadevan, J. Comments on the paper titled “Contact angle measurements of CO₂–water–quartz/calcite systems in the perspective of carbon sequestration”: A case of contamination? *International Journal of Greenhouse Gas Control* **2012**, *7* (0), 261-262.
- (53) London, G.; Carroll, G. T.; Feringa, B. L. Silanization of quartz, silicon and mica surfaces with light-driven molecular motors: construction of surface-bound photo-active nanolayers. *Organic & Biomolecular Chemistry* **2013**, *11* (21), 3477-3483.
- (54) Pedersen, K. S.; Christensen, P. L.; Shaikh, J. A. *Phase behavior of petroleum reservoir fluids*; CRC Press 2014.
- (55) Lander, L. M.; Siewierski, L. M.; Brittain, W. J.; Vogler, E. A. A systematic comparison of contact angle methods. *Langmuir* **1993**, *9* (8), 2237-2239.
- (56) Wolthers, M., Di Tommaso, D., Du, Z., de Leeuw, N. H. Calcite surface structure and reactivity: molecular dynamics simulations and macroscopic surface modelling of the calcite-water interface. *Physical Chemistry Chemical Physics* **2012**, *14*(43), 15145-15157.
- (57) Mahdi Jafari, S.; He, Y.; Bhandari, B. Nano-Emulsion Production by Sonication and Microfluidization—A Comparison. *International Journal of Food Properties* **2006**, *9* (3), 475-485.
- (58) Li, Y. V.; Cathles, L. M. Retention of silica nanoparticles on calcium carbonate sands immersed in electrolyte solutions. *Journal of Colloid and Interface Science* **2014**, *436* (0), 1-8.
- (59) Al-Yaseri, A. Z., Sarmadivaleh, M., Saedi, A., Lebedev, M., Barifcani, A., and Iglauer, S. N₂ + CO₂ + NaCl brine interfacial tensions and contact angles on quartz at CO₂ storage site conditions in the Gippsland basin, Victoria/Australia. *Journal of Petroleum Science and Engineering* **2015**, *129*, 58-62.
- (60) Sheppard, A.; Arns, J.-Y.; Knackstedt, M.; Pinczewski, W. V. Volume Conservation of the Intermediate Phase in Three-Phase Pore-Network Models. *Transp Porous Med* **2005**, *59* (2), 155-173.
- (61) Gharbi, O.; Blunt, M. J. The impact of wettability and connectivity on relative permeability in carbonates: A pore network modeling analysis. *Water Resources Research* **2012**, *48* (12), 1-14.

- (62) Iglauer, S.; Wüiling, W., Pentland, C.H., Al-Mansoori, S., and M.J. Blunt. Capillary trapping capacity of sandstones and sandpacks. *SPE Journal* 2011, 16(4), 778-783.
- (63) Nikolov, A.; Kondiparty, K.; Wasan, D. Nanoparticle Self-Structuring in a Nanofluid Film Spreading on a Solid Surface. *Langmuir* 2010, 26 (11), 7665-7670.
- (64) Täuber, D.; Trenkmann, I.; von Borczyskowski, C. Influence of van der Waals Interactions on Morphology and Dynamics in Ultrathin Liquid Films at Silicon Oxide Interfaces. *Langmuir* 2013, 29 (11), 3583-3593.
- (65) Zhuravlev, L. T.. The surface chemistry of amorphous silica. Zhuravlev model. *Colloids and Surfaces A: Physicochemical and Engineering Aspects* 2000, 173(1-3), 1-3.
- (66) Al-Yaseri, A. Z., Lebedev, M., Vogt, S. J., Johns, M. L., Barifcani, A., & Iglauer, S. Pore-scale analysis of formation damage in Bentheimer sandstone with in-situ NMR and micro-computed tomography experiments. *Journal of Petroleum Science and Engineering* 2015, 129, 48-57.
- (67) Salager, J.-L.; Marquez, N.; Graciaa, A.; Lachaise, J. Partitioning of Ethoxylated Octylphenol Surfactants in Microemulsion–Oil–Water Systems: Influence of Temperature and Relation between Partitioning Coefficient and Physicochemical Formulation. *Langmuir* 2000, 16 (13), 5534-5539.
- (68) Iglauer, S.; Wu, Y.; Shuler, P.; Tang, Y.; Goddard Iii, W. A. Alkyl polyglycoside surfactant–alcohol cosolvent formulations for improved oil recovery. *Colloids and Surfaces A: Physicochemical and Engineering Aspects* 2009, 339 (1-3), 48-59.
- (69) Metin, C.; Lake, L.; Miranda, C.; Nguyen, Q. Stability of aqueous silica nanoparticle dispersions. *Journal of Nanoparticle Research* 2011, 13 (2), 839-850.
- (70) Iglauer, S.; Wu, Y.; Shuler, P.; Tang, Y.; Goddard Iii, W. A. New surfactant classes for enhanced oil recovery and their tertiary oil recovery potential. *Journal of Petroleum Science and Engineering* 2010, 71 (1-2), 23-29.
- (71) Austad, T.; Shariatpanahi, S. F.; Strand, S.; Black, C. J. J.; Webb, K. J. Conditions for a Low-Salinity Enhanced Oil Recovery (EOR) Effect in Carbonate Oil Reservoirs. *Energy & Fuels* 2012, 26 (1), 569-575.
- (72) Castro Dantas, T. N.; Soares A, P. J.; Wanderley Neto, A. O.; Dantas Neto, A. A.; Barros Neto, E. L. Implementing New Microemulsion Systems in Wettability Inversion and Oil Recovery from Carbonate Reservoirs. *Energy & Fuels* 2014, 28 (11), 6749-6759.
- (73) Iglauer, S., Paluszny, A., & Blunt, M. J. Corrigendum to “Simultaneous oil recovery and residual gas storage: A pore-level analysis using in situ X-ray micro-tomography” [Fuel 103 (2013) 905–914]. *Fuel* 2015, 139, 780
- (74) Iglauer, S.; Wüiling, W., Pentland, C.H., Al-Mansoori, S., and M.J. Blunt. Capillary trapping capacity of sandstones and sandpacks. *SPE Journal* 2011, 16(4), 778-783.

Highlights

INTRODUCTION	2
EXPERIMENTAL METHODOLOGY	3
Materials	3
• Calcite surface preparation (surface cleaning and modification with silane).	4
• Preparation of nanofluids (different nanoparticles concentration in different brine concentration).	6
• Surface modification with nanofluid and contact angle measurements (Immersing of calcite surfaces in different nanofluids for different durations).	7
RESULTS AND DISCUSSION	8
• SEM and AFM images (Images taken before and after nano-modification) and EDS analysis (data have taken after nano-modification of the surface).	8
• Effect of exposure time on contact angle (contact angle was measured after different immersing time to investigate the effect of nanoparticles of the surface wettability with time).	10
• Adsorption phenomenon of nanoparticles on the surface (calcite surface was treated with different fluids after nano-modification to investigate the reversibility of adsorption process).	11
• Effect of brine concentration on contact angle (NaCl concentration was ranged between (0-20wt%) to investigate the effect electrolyte concentration on nanoparticles precipitation).	12
• Effect of nanoparticle concentration on contact angle (Nanoparticle concentration was ranged between (0-4wt%) to investigate the effect of silica nanoparticle concentration on contact angle).	14
• Efficiency of used nanofluid (Sustainability of silica nanoparticles was tested by measuring the contact angle after surface modification with fresh and pre-used nanofluid).	15

Graphical Abstract

